Observation of universal conductance-fluctuation crossovers in mesoscopic Li wires

J. S. Moon,* Norman O. Birge, and Brage Golding
Department of Physics and Astronomy and The Center for Fundamental Materials Research, Michigan State University, East Lansing, Michigan 48824-1116
(Received 6 June 1997)

We have measured the $1/f$ resistance noise of quench-condensed mesoscopic Li wires as a function of magnetic field over the range 0–9 T at low temperatures. The noise versus field reflects the crossover behavior of universal conductance fluctuations. Since Li has negligible spin-orbit scattering, the $1/f$ noise versus magnetic field shows two distinct reductions by factors of 2. The first results from the breaking of time-reversal invariance and the second from Zeeman splitting of the conduction-electron-spin degeneracy. In the experiment the thermal energy is larger than the Thouless energy; in this case the former energy governs the characteristic magnetic-field scale for the Zeeman crossover. In mesoscopic Li wires with finite spin-flip scattering due to magnetic impurities, the $1/f$ noise also shows a reduction by a factor of 2 in a weak magnetic field. At high magnetic field, however, the $1/f$ noise increases dramatically when the Zeeman splitting of the magnetic impurities is larger than the temperature. We analyze the data from both experiments quantitatively and find good agreement with theory. [S0163-1829(97)07247-0]

I. INTRODUCTION

The low-temperature electrical transport in weakly disordered metals has been well understood since the 1980s.[1] Conduction electrons diffuse on the scale of the elastic mean free path, l_e (typically tens of nanometers), which is determined by static impurities, lattice imperfections, grain boundaries, and sample dimensions. Processes that destroy phase coherence, such as inelastic electron-electron or electron-phonon scattering, and phase breaking from spin-flip scattering, occur much more rarely. At temperatures below 1 K the conduction electrons maintain phase coherence over length scales of the order of 1 μm. Quantum interference between multiply scattered paths of electrons on the scale of the phase-breaking length, L_ϕ, leads to quantum corrections to the electrical resistance, including the weak localization corrections to the average resistance[2] and the sample-specific universal conductance fluctuations (UCF).[3] The UCF manifest themselves as reproducible, but aperiodic, fluctuations in the conductance as a function of an external control parameter, such as magnetic field[4] or gate voltage.[5] In sufficiently small samples, the conductance fluctuations have an amplitude of order e^2/h that is nearly independent of sample size and shape, hence the name ''universal.'' One of the remarkable features of UCF is that their amplitude depends on the physical symmetries of the system under study, such as time-reversal symmetry or spin symmetry. Hence the UCF amplitude changes when the magnetic field exceeds certain values, and also varies in the presence or absence of magnetic impurities or spin-orbit scattering.

There have been two main theoretical approaches to calculate the magnitude of the UCF variance, $(\delta G)^2$, and its dependence on the various spin interactions including spin-orbit scattering, Zeeman splitting of the conduction-electron-spin degeneracy, and spin-flip scattering due to magnetic impurities. The original approach was based on a microscopic theory using impurity-averaged Green's functions.[6–9] Later, it was shown that the relative value of $(\delta G)^2$ (and also the exact value in one dimension) can also be obtained from random matrix theory, based on the statistical properties of the transmission matrix or the Hamiltonian.[10–13] The eigenvalues of those matrices obey the level repulsion property of the random matrix ensembles introduced by Wigner and Dyson in the context of nuclear physics:[14–16] the Gaussian orthogonal ensemble (GOE) for a system with time-reversal and spin symmetry, the Gaussian unitary ensemble (GUE) when time-reversal symmetry is broken, and the Gaussian symplectic ensemble (GSE) in the limit of strong spin-orbit scattering. The theoretical prediction for the UCF variance is

$$(\delta G)^2 \approx \frac{2}{15}\left(\frac{e^2}{h}\right)^2 \frac{ks^2}{\beta}, \tag{1}$$

where k is the number of independent eigenvalue sequences of the transmission matrix or Hamiltonian, s is the eigenvalue degeneracy, and β is equal to 1, 2, or 4 for the GOE, GUE, and GSE, respectively. Equation (1) is an equality for one-dimension; for higher dimensions the exact numerical prefactor must be obtained from Green's function calculations.[7]

Application of a magnetic field or addition of spin-orbit (SO) scattering changes the physical symmetry of a system, resulting in the variation of the UCF magnitude.[11] A system with small spin-orbit scattering at zero magnetic field has the highest symmetry ($\beta=1$, $k=1$, $s=2$), with UCF variance of $\approx(e^2/h)^2$ given by Eq. (1). With application of a magnetic field, one should observe two distinct reductions of $(\delta G)^2$ by factors of 2. The first comes from breaking of time-reversal invariance of the electron orbital motion ($\beta=1\rightarrow\beta=2$) and the second is due to lifting of the spin degeneracy of the conduction electrons (the electron spin degeneracy, $s=2\rightarrow s=1$) and producing two (spin-up and spin-down) statistically independent eigenvalue sequences ($k=1\rightarrow k=2$). In a system with strong spin-orbit scattering, the spin-rotation symmetry is already broken at zero magnetic field ($\beta=4$) but not the time-reversal symmetry, hence $(\delta G)^2$ is

a factor of 4 smaller than in a low SO scattering material. Application of a magnetic field in this system lifts the two-fold Kramers degeneracy associated with the time-reversal invariance ($s=2\rightarrow s=1$; $\beta=4\rightarrow\beta=2$), leading to a single factor of 2 reduction in $(\delta G)^2$ as a function of field.

There have been a series of experiments to verify these predictions. The initial experiments[4,5] established the near-universal amplitude of the conductance fluctuations, but did not address the more subtle issue of the different universality classes implicit in Eq. (1). A study of the UCF-enhanced $1/f$ noise versus magnetic field in Bi films clearly confirmed the factor of 2 reduction of $(\delta G)^2$ versus field in the strong spin-orbit regime.[17] The factor of 4 change in $(\delta G)^2$ associated with the relative size of the spin-orbit scattering length and the phase-breaking length has also been observed.[18] Until now, there has been no clear verification of the two reductions of $(\delta G)^2$ as a function of magnetic field starting from the *fully symmetric, low spin-orbit scattering system* (GOE). The interpretation of an earlier measurement[19] of the UCF crossovers in a low spin-orbit scattering system is suspect, because the magnetic-field scale associated with the Zeeman crossover reported in Ref. 19 is not consistent with the experimental and theoretical results presented here.

Another issue addressed in this paper is the dependence of $(\delta G)^2$ on the spin-flip scattering rate. Frequent flipping of the electron spin states, for example, due to magnetic impurities, breaks the phase coherence and suppresses $(\delta G)^2$ compared to the case without magnetic scatterers. When the Zeeman energy of the magnetic scatterers is larger than the temperature, the spin-flip scattering will be suppressed, hence the value of $(\delta G)^2$ without magnetic impurities is recovered.[20] Several experiments[21–23] unraveled this high-field behavior of $(\delta G)^2$ in a system with magnetic impurities. An issue not yet shown experimentally is whether $(\delta G)^2$ in the presence of dilute magnetic scatters is reduced by an exact factor of 2 in a weak magnetic field. In the Green's-function approach to the theory,[6–9] there are contributions to $(\delta G)^2$ arising from two classes of diagrams, Cooperon and diffuson. The two contributions are equal at zero field, while the Cooperon contribution is suppressed in a weak field. Since spin-flip scattering reduces both contributions equally in the limit of weak SO scattering, application of a weak magnetic field should reduce $(\delta G)^2$ by a factor of 2.

To address the issues discussed above, we need a reliable experimental method to obtain the relative value of the UCF variance, $(\delta G)^2$, as a function of magnetic field. The traditional method of measuring static conductance fluctuations versus magnetic field (the ''magnetofingerprint'') is inappropriate because we need the value of $(\delta G)^2$ at fixed field. Warming up the sample repeatedly to produce different microscopic configurations of the scattering centers is not practical. Fortunately, in disordered metals, impurities or scattering centers rearrange themselves spontaneously at low temperature by quantum-mechanical tunneling.[24] These rearrangements give rise to dynamic conductance fluctuations via UCF.[25,26] In samples large enough so that many mobile defects contribute to the conductance fluctuations, one observes $1/f$ noise in the conductance due to the broad distribution of tunneling rates in disordered metals.[17,27] The total conductance change (the square root of the noise power integrated over the experimental bandwidth) in metals is typically much less than e^2/h; the noise is referred to as ''unsaturated.'' Nevertheless, the relative magnitude of the noise as a function of magnetic field reflects the universal ratios implicit in Eq. (1).[8,17]

In this paper, we describe $1/f$ noise measurements on quench-condensed mesoscopic Li wires, with a thorough presentation of UCF theory. We have chosen the lightest metal, lithium, for its low spin-orbit scattering rate.[28] We address several important issues regarding UCF's in the low spin-orbit scattering regime, both with and without spin-flip scattering. In an experiment carried out in a sample with negligible spin-dependent scattering, we clearly observe two distinct reductions of the $1/f$ noise power as a function of magnetic field, as predicted by Eq. (1). We evaluate the complete theoretical expression describing both reductions and find good agreement with our data. Some of these results have already appeared,[29] but without the full theory. In our experiment the thermal energy k_BT is larger than the Thouless energy E_c. Under this condition, we find both experimentally and theoretically that the magnetic-field scale for the electronic Zeeman crossover is $B_{c2}\cong 2.7k_BT/g\mu_B$, much larger than the value of $B_{c2}\cong E_c/g\mu_B$ predicted earlier.[8] In Sec. VII, we show $1/f$ noise measurements as a function of magnetic field in a sample with low spin-orbit scattering but with significant spin-flip scattering. We indeed observe a factor of 2 reduction in the $1/f$ noise with an application of magnetic field, confirming the theoretical prediction that spin-flip scattering suppresses equally the Cooperon and diffusion contributions to the conductance fluctuations. At high magnetic field, we observe a dramatic increase in the noise, consistent with the previous observations that spin-flip scattering is suppressed in a high magnetic field.[21–23]

II. EXPERIMENT

For minimal spin-orbit scattering, we have fabricated mesoscopic samples made of lithium. The sample dimensions are in the quasi-1D regime ($t,W<L_\phi<L$, where t, W, and L are the sample thickness, width, and length, respectively), because this restricted geometry further enhances the noise power via UCF.[25] L_ϕ is typically of the order of 1 μm at 1 K, so samples with submicron transverse dimensions were fabricated using electron-beam lithography on silicon substrates. The samples were patterned with five leads for measurement in a Wheatstone bridge circuit.

Since lithium metal is very reactive in air, it must be handled in an inert gas (He or Ar) atmosphere or in a high vacuum. We evaporate lithium thermally onto a cold substrate kept at 4.2 K, which yields contamination-free disordered films. Quench-condensation of the Li films through the submicron mask, combined with *in situ* measurements, requires major changes of conventional lithography because the final ''lift-off'' process cannot be carried out. The mask must provide electrical isolation between the material deposited on the substrate and that on the mask surface. Also, the mask must be thermally resistant during the evaporation and thermal cycling. Licini *et al.*[30] used a Cr metal stencil fabricated by ''canyon'' lithography.[31] In our work we also utilize a trilayer lithography, based on a PMMA/metal/copolymer structure to make a submicron metal stencil.

Here, a 50-nm-thick layer of aluminum is used for the metal layer because it can be wet-etched easily. The copolymer layer at the bottom provides electrical isolation between the metal stencil and the deposited sample.

After the Li films are quench-condensed, they are annealed at 35–40 K to minimize long-term drift in their resistance. The resistance and $1/f$ noise were measured with a low-frequency (510 Hz) ac bridge method,[32] with a liquid-nitrogen cooled step-up transformer to increase the sample-to-preamplifier noise ratio. To compensate for possible background fluctuations during the $1/f$ noise measurement, the total noise ($1/f$ noise+background) and the background were measured simultaneously with a two-phase digital lock-in amplifier. All the electrical leads to the sample are RF filtered at the entry to the cryostat, and again at the entry to the shielded room. A magnetic field perpendicular to the samples is provided by a 9-T superconducting magnet.

III. MAGNETORESISTANCE AND WEAK LOCALIZATION

In a quasi-1D wire, the weak localization (WL) contribution to the resistance is given by[33]

$$\frac{\Delta R}{R}=\frac{e^2}{\pi\hbar}\frac{R}{L}\{\tfrac{3}{2}[L_{\ln}^{-2}+\tfrac{4}{3}L_{so}^{-2}+\tfrac{2}{3}L_{sf}^{-2}+L_B^{-2}]_{\text{triplet}}^{-1/2}-\tfrac{1}{2}[L_{in}^{-2}+2L_{sf}^{-2}+L_B^{-2}]_{\text{singlet}}^{-1/2}\},\quad(2)$$

where L_{in}, L_{so}, and L_{sf} are the inelastic, spin-orbit, and spin-flip scattering lengths, respectively, and where the effect of magnetic field is expressed in terms of a 1D magnetic length, $L_B=(\sqrt{3}/2\pi)(h/e/BW)$. Note that the definition of the phase-breaking length, L_ϕ, is somewhat ambiguous in the presence of spin-flip scattering because that process contributes differently to phase breaking in the singlet and triplet terms of Eq. (2). Strong spin-orbit scattering suppresses the triplet term, and hence changes the sign of the magnetoresistance at low field from negative to positive. Strong spin-flip scattering suppresses both terms, hence it reduces the magnitude of the WL correction. Hence, the WL correction in the magnetoresistance provides a tool to characterize our Li films in terms of spin-dependent scattering and inelastic scattering.

We measured the magnetoresistance versus temperature of six samples, described in Table I. Samples 1 and 2 were evaporated from a Ta filament, whereas samples 3–6 were evaporated from a Ni-Cr filament. We will show below that the samples fabricated with the Ni-Cr filament exhibit large spin-flip scattering, presumably due to Cr impurities in the films.[34] Figure 1 shows the magnetoresistance versus temperature obtained from sample 1, which is quasi-1D. In our experimental temperature range, the magnetoresistance is always negative, implying that the spin-orbit scattering is relatively weak in the sample. The solid lines in Fig. 1 are least-squares fits to the quasi-1D WL theory assuming no spin-dependent scattering ($L_{so}=L_{sf}=\infty$, hence $L_\phi=L_{in}$). From these fits, we obtain an estimate of the phase breaking length, L_ϕ, at each temperature. Its temperature dependence can be expressed as $L_\phi^{-2}=0.085T^2+0.20$ (where L_ϕ is in μm and T is in K) as shown in Fig. 2. Analysis of the temperature dependence of L_ϕ for all the samples, both 1D and 2D, assuming no spin-dependent scattering, is shown in Fig. 2. For each sample, the data fall on a straight line, $L_\phi^{-2}=AT^2+B$. This power-law behavior in Li films has been reported previously[30] over a wide range of temperature, although the origin of the T^2 dependence is not understood. Samples 3–6 have large values of the intercept B, in contrast to samples 1 and 2. Figure 3 shows magnetoresistance data from sample 3, where the WL corrections saturate noticeably as the temperature is decreased, which can arise from residual spin-flip scattering as shown by Eq. (2). Determination of the spin-dependent scattering rates is difficult from the fit of the magnetoresistance data at a single temperature, due to the large number of parameters in Eq. (2). For samples 3 and 4, we carried out global fits of the magnetoresistance data at all temperatures to Eq. (2). In each global fit, we assume $L_{in}^{-2}=\alpha T^2$, using as fitting parameters the temperature-independent length scales L_{so} and L_{sf}, as well as the constant α. The solid lines in Fig. 3 present our global fit to all magnetoresistance data for sample 3, with the values $L_{so}=0.46\ \mu$m, $L_{sf}=0.37\ \mu$m, and $\alpha=0.56\ \text{K}^{-2}\ \mu\text{m}^{-2}$. Application of the global fit to sample 4 yields $L_{so}=0.26\ \mu$m,

TABLE I. Sample parameters. l_e was determined from the resistivity using free-electron theory. L_{in} was determined by fitting magnetoresistance data with Eq. (2), labeled MR, or $1/f$ noise power vs magnetic field with Eq. (4), labeled $1/f$. From samples 3 and 4, $L_{so}=0.46$ and 0.26 μm, and $L_{sf}=0.37$ and 0.23 μm, respectively (see the text). For sample 1, the table shows L_ϕ, not L_{in}, determined with $L_{so}=L_{sf}=\infty$.

						L_{in} (μm)			
Sample	L	W	t	$R_\square$	l_e	$T=1.6$ K		$T=4.2$ K	
No.	(μm)	(μm)	(nm)	(Ω)	(nm)	MR	$1/f$	MR	$1/f$
1	20	0.45	54	0.45	40	1.5	1.0	0.75	0.65
2	20	0.2	33	0.9	32				
3	20	0.11	13	5.7	13	0.83	0.65	0.34	0.35
4	20	0.12	9	11.5	4.4	0.74	0.7	0.28	0.27
5	5800	205		7.8					
6	5800	205		1.7					

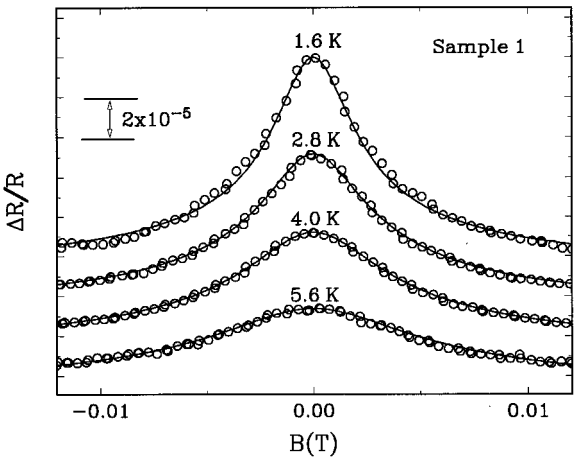

FIG. 1. Magnetoresistance data from sample 1 at temperatures 1.6, 2.8, 4.0, and 5.6 K. The solid lines are fits to quasi-1D weak-localization theory with no spin-dependent scattering.

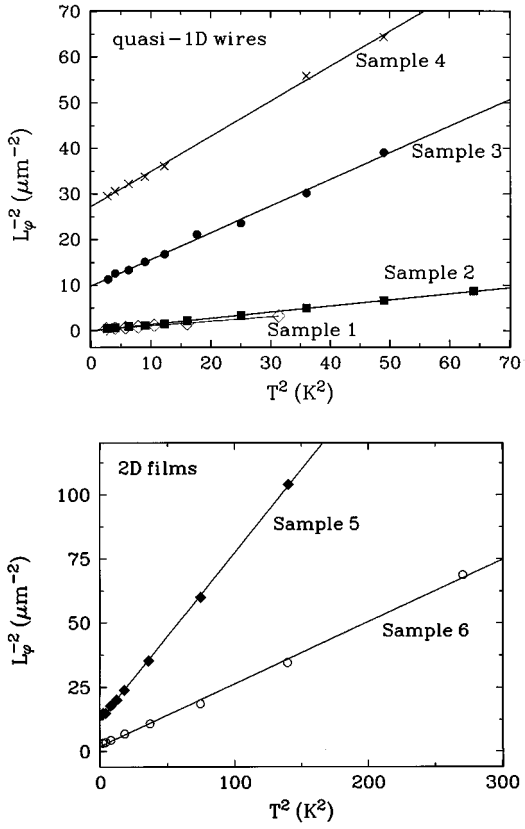

FIG. 2. The electron phase breaking length vs temperature obtained from the weak-localization fits to low-field magnetoresistance for quasi-1D wires (upper panel) and for 2D films (lower panel). The straight lines are linear least-squares fits to the data.

$L_{sf}=0.23\ \mu$m, and $\alpha=0.71\ \mathrm{K}^{-2}\ \mu\mathrm{m}^{-2}$. In these samples, electrons lose phase coherence mostly due to strong spin-flip scattering.

Mohanty, Jariwala, and Webb[35] have recently shown that an observed saturation of L_ϕ at low temperature can arise from an intrinsic quantum-mechanical dephasing process.

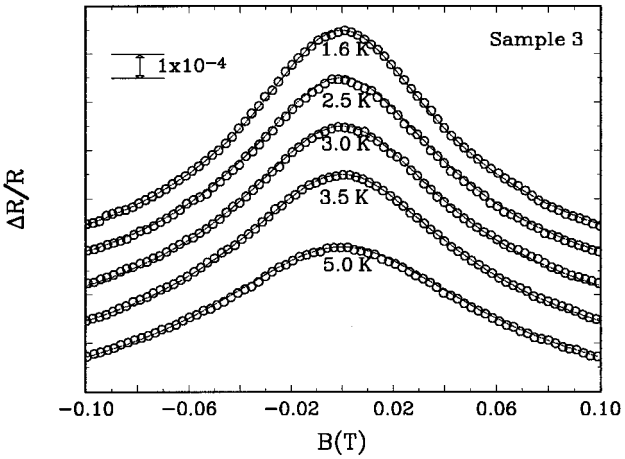

FIG. 3. Magnetoresistance data from sample 3 (with residual spin-flip scattering) at temperatures 1.6, 2.5, 3.0, 3.5, and 5.0 K. The solid lines are global fits (see text) to quasi-1D weak-localization theory.

Using Eq. (2) from their paper, we find that the phase-breaking length in all our samples is considerably shorter than the intrinsic limit, lending further support to our interpretation in terms of spin-dependent scattering. In addition, the presence of strong spin-flip scattering in sample 3 is consistent with our observation of a strong increase in the noise at high field in that sample, to be discussed in Sec. VI.

IV. 1/f NOISE AND UCF

As discussed earlier, the calculation of the UCF amplitude can be performed within the framework of random matrix theory, with the result given by Eq. (1), or by using the formalism of impurity-averaged Green's functions. With the latter method, one finds that the fluctuations arise from two classes of diagrams, called the Cooperon or ''particle-particle'' channel and the diffuson or ''particle-hole'' channel, which give equal contributions at zero magnetic field.[18] A simple way to view the various UCF reduction factors is to describe the UCF variance in terms of the spin variables of the channels.[36] The spin variables are total spin J and its projection M_z of electron and hole for the diffuson channel, and of electron and electron for the Cooper channel. If we rewrite each channel in terms of spin-singlet ($J=0$, $M_z=0$) and spin-triplet ($J=1$, $M_z=\pm1,0$) terms, then the UCF variance is given by

$$(\delta G)^2=[\tfrac{1}{4}(\delta G_s(B))^2+\tfrac{3}{4}[\delta G_t(B,L_{so})]^2]_{pp}+\left[\tfrac{1}{4}(\delta G_s)^2+\tfrac{1}{4}\sum_{M_z}[\delta G_t(M_z g\mu_B B,L_{so})]^2\right]_{ph}, \tag{3}$$

where δG_s and δG_t stand for the conductance fluctuations of the singlet and triplet part, respectively, and pp and ph mean the particle-particle and particle-hole channel, respectively. Strong spin-orbit scattering ($L_{so}\to0$) suppresses the triplet contribution in both channels, leading to a factor of 4 reduction in the UCF variance. The effect of magnetic field arises in two different ways: an orbital effect in the Cooperon channel and a spin effect in the diffuson channel. Application of a weak magnetic field suppresses the Cooperon channel completely (both singlet and triplet), while the diffuson channel remains unaffected, hence the UCF variance is reduced by a factor of 2 whether the spin-orbit scattering is strong or not. At high magnetic field, if the spin-orbit scattering is weak, the effect of Zeeman splitting of the conduction electron spin degeneracy can be observed due to the suppression of the $M_z=\pm1$ triplet parts in the diffuson channel. The singlet and the $M_z=0$ part of the triplet contribution remain, hence the Zeeman splitting results in a second factor of 2 reduction of the UCF variance.

V. ORBITAL EFFECT ON UCF

We have measured the 1/f resistance noise of several quasi-1D samples as a function of an applied perpendicular magnetic field. Figure 4(a) shows the 1/f noise power, normalized to its value at zero field, from sample 3. As predicted by Eq. (3), the noise power at low magnetic field is reduced by a factor of 2. A reduction of 1/f noise by a full

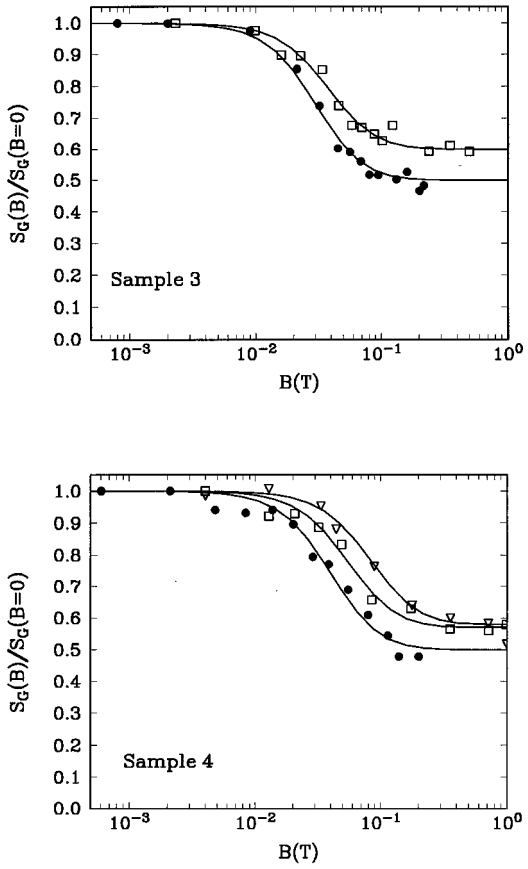

FIG. 4. Conductance noise power as a function of the perpendicular magnetic field, normalized by its zero-field value. The data for sample 3 (upper panel) are taken at temperatures 1.6 (●) and 4.2 K (□). The data for sample 4 (lower panel) are taken at temperatures 1.6 (●), 4.2 (□), and 10 K (▽). The solid lines are fits to Eq. (4), as discussed in the text.

factor of 2 is observed at 1.6 K, but the noise at 4.2 K does not quite drop by a full factor of 2 and levels off at 0.6. Figure 4(b) shows a similar behavior for sample 4. We believe that this leveling off in the noise power is due to a small contribution of local-interference-type noise, which is magnetic-field independent.[37,38]

The theoretical expression for the $1/f$ noise crossover function due to the suppression of the Cooper channel has been calculated by Stone for the case of 2D films.[8] He showed that the characteristic field scale, B_{c1}, corresponds approximately to one flux quantum (h/e) over a phase-coherent area. To compare our $1/f$ noise data obtained in quasi-1D samples with theory, we have calculated the 1D noise crossover function in two different ways. First, we have utilized[29] an approximate analytical expression for the field-correlation function calculated by Beenakker and van Houten.[39] We have also evaluated numerically the complete theoretical expression for the 1D noise crossover, described in the Appendix.[40] We found that the difference between the approximate analytical and the exact numerical expressions is negligible. From the evaluation of the noise crossover function, $\nu_1(B)$, we are able to determine the characteristic field scale, B_{c1}, explicitly in the quasi-1D regime. The result is $B_{c1}=A(h/e/L_\phi W)$, where the numerical constant A depends weakly on the ratio of L_ϕ and $L_T=\sqrt{\hbar D/k_B T}$, where

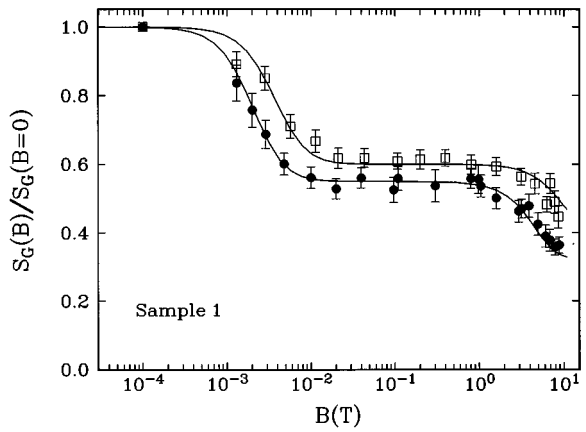

FIG. 5. Conductance noise power as a function of magnetic field at 1.6 (●) and 4.2 K (□) from sample 1. The data are normalized by the noise power at zero-field value. The solid lines are fits to Eq. (4), including both the low-field crossover [Eq. (A8), due to suppression of the Cooperon channel] and the high-field crossover [Eq. (A9), due to Zeeman splitting of the conduction-electron-spin degeneracy].

$D=v_F l_e/3$ is the electronic diffusion constant. The constant A lies between 0.21 for $L_\phi \gg L_T$ and 0.16 for $L_\phi \ll L_T$.

In the actual fit to our data, we include an extra parameter c to account for the small local-interference-type noise present in our sample. So, the function we use is

$$\frac{S_G(B)}{S_G(B)} = c + (1-c)\,\nu(B), \tag{4}$$

where for $\nu(B)$ we use the function $\nu_1(B)$ valid at low field, given by Eq. (A8) in the Appendix. The solid lines in Figs. 4(a), 4(b), and in the low-field part of Fig. 5 show our fits of Eq. (4) to the data. In the fit to the noise versus magnetic field for samples 3 and 4, we used the values of L_{so}, and L_{sf} determined from the magnetoresistance analysis. Our best-fit parameters for sample 3 are $c=0$ and 0.2 and $L_{in}=0.65$ and 0.34 μm at 1.6 and 4.2 K, respectively. The latter are very close to the values 0.8 and 0.35 μm obtained from magnetoresistance measurements. The fit parameters for sample 4 are $c=0$, 0.14, and 0.16 and $L_{in}=0.7$, 0.27, and 0.12 μm at 1.6, 4.2, and 10 K, respectively. Therefore, the noise measurements from samples 3 and 4 provide experimental evidence that a small magnetic field suppresses conductance fluctuations by a factor of 2 even in the presence of significant spin-flip scattering. Sample 1, with little spin-flip scattering, also exhibits a reduction of noise at low field, as shown in Fig. 5. The solid lines at low field in Fig. 5 are fits with $c=0.1$ and 0.2, and $L_{in}=1.0$ and 0.65 μm at 1.6 and 4.2 K, respectively. The values of L_{in} for sample 1 are somewhat smaller than those obtained from magnetoresistance data: $L_{in}=1.5$ and 0.77 μm at 1.6 and 4.2 K, respectively. A similar discrepancy has been observed in 2D Ag films[38] and we believe it indicates that the dominant inelastic scattering process at low temperature, probably electron-electron scattering with small energy transfer,[41] contributes to phase-breaking more strongly in the case of UCF than in the case of WL.[42]

VI. ZEEMAN SPLITTING OF CONDUCTION ELECTRONS

The noise data in Fig. 5 show a second reduction by a factor of 2 at strong magnetic field, as predicted by Eqs. (1) and (3). This reduction in UCF arises from Zeeman splitting of the spin degeneracy of the conduction electrons. The solid lines at high field in Fig. 5 present our numerical evaluation of the electronic Zeeman crossover, given again by Eq. (4), but now for $\nu(B)$ we use the expression $\nu_2(B)$ valid at high field and given by Eq. (A9) in the Appendix. The theory is in excellent agreement with the data. We emphasize that there are no free parameters in the theory—the constant c in Eq. (4) was already determined by the fit to the low-field data. The characteristic magnetic field scale for the Zeeman crossover is $B_{c2} \cong 2.7 k_B T / g \mu_B$.

Understanding of the energy scale governing B_{c2} has proven problematic. Stone claimed that B_{c2} for unsaturated UCF's is determined by the Thouless energy, $E_c = hD/L_\phi^2$, rather than by the temperature.[8] Feng's published result[9] only covered the case $k_B T < E_c$, whereas the situation more often encountered in experiment is $k_B T > E_c$. Experimentally, Debray *et al.*[19] measured the static variation of conductance in a quasi-1D GaAs/Al_xGa_{1-x}As heterostructure as a function of gate voltage at several values of magnetic field at 1.3 K. After a first reduction of $(\delta G)^2$ by a factor of 2 below $B \sim 10$ G (confirmed by one data point at very low field), they reported the observation of a second factor of 2 reduction at $B \sim 0.07$ T. They estimated the Thouless energy as $E_c/k_B \approx 88$ mK and concluded that B_{c2} is determined by the Thouless energy. However, when $k_B T > E_c$, which is the case both for our experiment and that of Debray *et al.*, we conclude that B_{c2} is determined by $k_B T$. Numerical evaluation of the high-field crossover expression given in the Appendix yields $B_{c2} \cong 2.7 k_B T / g \mu_B$ for the case $k_B T \gg E_c$, and $B_{c2} \cong 0.56 E_c / g \mu_B$ when $k_B T \ll E_c$. We use the free-electron value of the g factor $(=2)$ and we find $B_{c2} = 3.9$ T for $T = 1.9$ K, in excellent agreement with the experimental data shown in Fig. 5. We can only guess why the experimental results of Debray *et al.* are not consistent with this picture: (1) the magnetoresistance data did not fit to weak localization theory, which provides the phase-breaking length and an estimate of the Thouless energy; (2) there was only one data point showing the first reduction of the UCF by a factor 2—thus if the zero-field data point were incorrect, then the second reduction observed might actually correspond to the suppression of the Cooper channel, rather than to the Zeeman splitting as the authors claimed; (3) a major difficulty in extracting the energy scale for B_{c2} from the experiment on the GaAs/Al_xGa_{1-x}As structure lies in the fact that several values of the g factor, ~ 0.4 (Ref. 43) and 13 (Ref. 44), as well as a magnetic-field dependence of the g factor in GaAs/Al_xGa_{1-x}As heterostructures have been reported.

VII. ZEEMAN SPLITTING OF MAGNETIC IMPURITIES

The discussion in the previous section concerned the Zeeman splitting of the conduction electron spin degeneracy. Another interesting issue is the dependence of $(\delta G)^2$ on magnetic field due to Zeeman splitting of magnetic impurities. Figure 6 shows the magnetic-field dependence of the relative $1/f$ noise power up to 9 T obtained from sample 3.

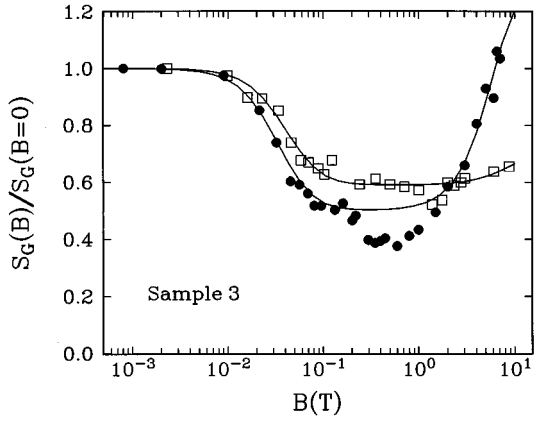

FIG. 6. Conductance noise power as a function of magnetic field at 1.6 (●) and 4.2 K (□) from sample 3. The reduction of noise at low field is discussed in Fig. 4(a). The noise data at high-field are fit to the paramagnetic impurity model [Eq. (5)] with a single value of magnetic moment, as discussed in the text.

The noise power increases with field dramatically when $B > 0.5$ T at 1.6 K, and slightly when $B > 1$ T at 4.2 K. This behavior is in contrast to the reduction we observe in sample 1, which is due to the conduction electron Zeeman splitting effect.

A probable explanation of the behavior shown in Fig. 6 is based on the observation that there is finite residual spin-flip scattering in the sample, as shown in the magnetoresistance measurement. In a system with dilute paramagnetic impurities, spin-flip scattering is an additional phase-breaking process, which suppresses the conductance fluctuations. When the Zeeman splitting of the impurity spin states exceeds $k_B T$, $(\delta G)^2$ will be recovered due to the alignment of the magnetic impurity spins and the suppression of spin-flip scattering. The magnetic-field scale is $k_B T/\mu_{\rm imp}$, which corresponds to 1.1 and 3.1 T at 1.6 and 4.2 K, respectively if we assume that the magnetic moment of the impurity is $\mu_{\rm imp} = 2\mu_B$. These estimated magnetic-field scales are close to the experimental observations.

To analyze the data quantitatively, the spin-flip scattering needs to be incorporated into UCF. Benoit *et al.*[45] calculated $(\delta G)^2$ in a system with paramagnetic impurities at high magnetic field, assuming that (1) only the lowest two magnetic energy levels of the impurity would be important, so that the magnetic impurity could be treated as spin $\frac{1}{2}$, and (2) the magnetic scattering rate would be proportional to $P_u P_d$, where P_u and P_d are the probabilities of the spin-$\frac{1}{2}$ impurity being in the up or down state. The magnetic-field dependence of the spin-flip scattering rate can be incorporated into the total phase-breaking rate:

$$L_\phi^{-2} = L_{\rm in}^{-2} + \frac{L_{\rm sf}^{-2}(B=0)}{\cosh^2\left(\dfrac{\mu_{\rm imp} B}{K_B T}\right)}. \tag{5}$$

A theoretical expression for the noise with spin-flip scattering can be derived in a straightforward manner, similar to the calculations of the noise crossover function in the Appendix. The additional SO scattering due to the dilute magnetic impurities is still negligible as shown in the negative magne-

toresistance. Thus, the theoretical expression depends on the quantities $L_{\rm in}$, $L_{\rm sf}(B=0)$, and $\mu_{\rm imp}$. The solid lines at high field in Fig. 6 show our fits to the theoretical expression with only a single fit parameter, $\mu_{\rm imp}=0.7\mu_B$, where we used the values of $L_{\rm in}$ obtained from the low-field fit to noise versus magnetic field, and $L_{\rm sf}(B=0)$ determined by the low-field magnetoresistance. Here, we assume that the effect on UCF of Zeeman splitting the conduction electron spins is negligible because there is strong spin-flip scattering, $L_{\rm sf}/L_{\rm in}\sim 0.5$ at 1.6 K, which breaks the electron spin symmetry. Surprisingly, the simple theoretical function matches the data fairly well and describes both temperature and field dependence of the noise power at high field in Fig. 6. Even though not all of the features in the noise data are explained from the simple model, the noise measurement provides a compelling picture of how spin-flip scattering changes the magnitude of conductance fluctuations.

VIII. SUMMARY

We have studied quantum transport in the *low spin-orbit scattering limit* by measuring UCF-enhanced $1/f$ noise as a function of magnetic field and the weak-localization correction to the average conductance in mesoscopic Li wires and films. In samples with low spin-flip scattering, the $1/f$ noise power drops twice as a function of magnetic field, which confirms the theoretical predictions in the low spin-orbit scattering limit. The first drop, at low field, is fit by a theoretical calculation of the suppression of the Cooper channel contribution to UCF, with the crossover field scale determined by one flux quantum over the phase coherent area. The second drop, at high field, arises due to Zeeman splitting of the conduction-electron-spin degeneracy. The theoretical crossover function for the high-field crossover agrees well with the data, with no adjustable parameters. Our results show that when the sample temperature is larger than the Thouless energy, the magnetic-field scale for the electronic Zeeman crossover is determined by the larger energy scale. This is different from previous theoretical[8] and experimental[19] work, where the field scale was presumed to be determined by the Thouless energy alone.

We also studied the effect of spin-flip scattering on UCF in the low spin-orbit scattering regime. In samples with magnetic impurities, the amplitude of conductance fluctuations increases in a dramatic way at high magnetic field where the Zeeman energy of magnetic impurities is larger than the temperature. From the fact that the noise power is reduced by an exact factor of 2 with application of a weak magnetic field, we confirmed the theoretical prediction that the spin-flip scattering suppresses the conductance fluctuations equally in the Cooperon and diffusion channels.

ACKNOWLEDGMENTS

We are grateful to the late Shechao Feng for sending us his calculations of the 1D UCF crossover function, including the effect of spin degeneracy and Zeeman splitting. We have also benefited from discussions with H. Fukuyama, A. D. Stone, and P. McConville, and we are grateful to E. Scherr for a critical reading of the manuscript. We acknowledge the NSF for support of this work under Grants Nos. DMR-9321850 and DMR-9312544.

APPENDIX

In this appendix, we describe the calculation of the 1D crossover functions used to fit our data of UCF-enhanced $1/f$ noise versus magnetic field. The conceptual starting point is Eq. (3), which shows the contributions to UCF from the different spin ($J=0$ and $J=1$) and Green's-function (Cooperon and diffuson) channels. For our $1/f$ noise experiments, we need the analogous formula for unsaturated conductance fluctuations, i.e., fluctuations with amplitude much less than e^2/h. We follow the procedure of Al'tshuler and Spivak,[26] which is described in detail for the 2D case by Stone.[8] Each of the quantities $(\delta G)^2$ in Eq. (3) should be replaced by the variance of unsaturated conductance fluctuations, $(\delta G')^2$:

$$\delta g'^2=\left[\tfrac{1}{4}(\delta g_s'(B))^2+\tfrac{3}{4}(\delta g_t'(B,L_{\rm so}))^2\right]_{\rm pp} +\left[\tfrac{1}{4}(\delta g_s')^2+\tfrac{1}{4}\sum_{M_z}(\delta g_t'(M_z g\mu_B B,L_{\rm so}))^2\right]_{\rm ph}, \tag{A1}$$

where s and t stand for singlet ($J=0$) and triplet ($J=1$, $M_z=-1$, 0, or 1), and pp and ph stand for particle-particle (Cooperon) and particle-hole (diffuson) contributions. Each term in Eq. (A1) is of the form

$$\delta g'^2(B,T)=-\frac{4s^2}{\pi^2}\int\frac{d\Delta E}{2k_BT}K\left(\frac{\Delta E}{2k_BT}\right)\frac{d}{d(1/\tau_\phi)}\times F_0(\Delta E,B), \tag{A2}$$

where $K(x)=(x\coth x-1)/\sinh^2 x$, s is the spin degeneracy, and $F_0(\Delta E,B)$ is the $T=0$ energy correlation function, which is a sum over powers of eigenvalues λ:

$$F_0(\Delta E,B)=\sum_m\left[\frac{1}{|\lambda|^2}+\tfrac{1}{2}\,{\rm Re}\left(\frac{1}{\lambda^2}\right)\right]. \tag{A3}$$

The normalized (dimensionless) eigenvalues for the Cooperon (pp) channel, calculated by Lee, Stone, and Fukuyama,[7] are given in the weak spin-orbit scattering limit as

$$\lambda_{\rm pp}(m,\Delta E,B)=m^2+\left(\frac{L}{\pi L_\phi}\right)^2+\frac{4}{3}\left(\frac{L}{L_\phi}\right)^2\left(\frac{BL_\phi W}{h/e}\right)^2-i\,\frac{\Delta E}{\pi^2\hbar D/L^2}, \tag{A4}$$

where m is an integer, ΔE is the energy difference between two Green's functions. The effect of Zeeman splitting of conduction electrons on UCF was calculated by Stone[8] and by Feng.[9,40] The normalized eigenvalues of the diffuson channel are given by

$$\lambda_{\rm ph}(m,\Delta E,M_z,B)=m^2+\left(\frac{L}{\pi L_\phi}\right)^2-i\,\frac{(\Delta E+M_z g\mu_B B)}{\pi^2\hbar D/L^2}. \tag{A5}$$

Spin-dependent scattering is incorporated into Eqs. (A4) and (A5) following Chandrasekhar *et al.*[36] The singlet (s) and triplet (t) channels each have their own phase-breaking length:

$$L_{\phi,s}^{\mathrm{UCF}}=[L_{\mathrm{in}}^{-2}+L_{\mathrm{sf}}+L_{\mathrm{st}}^{-2}(B)]^{-1/2},$$

$$L_{\phi,t}^{\mathrm{UCF}}=[L_{\mathrm{in}}^{-2}+L_{\mathrm{sf}}^{-2}(B)+\tfrac{4}{3}L_{\mathrm{so}}^{-2}]^{-1/2}. \quad \text{(A6)}$$

To get from $(\delta g')^2$ to the crossover function for $1/f$ noise, we need to assume that the number of mobile defects in the sample that contribute to the noise within the bandwidth of the experiment, is unchanged by the magnetic field.[46] Then the $1/f$ noise crossover function, $\nu(B)$, is given by

$$\nu(B)=\frac{\delta g'^2(B)}{\delta g'^2(0)}. \quad \text{(A7)}$$

Equations (A1)–(A7) give the complete noise crossover function, valid at all magnetic fields. As shown in Fig. 5, there are two noise crossovers as a function of magnetic field for the case of negligible spin-dependent scattering. The first arises from the orbital effect, which kills the Cooper channel contribution to UCF, while the second arises from the Zeeman effect in the diffuson channel. Since the magnetic-field scales for the two crossovers are spaced far apart, we can fit the data one piece at a time. At low field, the diffuson contribution to $\nu(B)$ is constant (and equal to $\frac{1}{2}$), and the crossover occurs as the Cooperon contribution is suppressed with field. Hence the low-field crossover function takes the form

$$\nu_1(B)=\tfrac{1}{2}\left(1+\frac{\delta g_{\mathrm{pp}}'^2(B)}{\delta g_{\mathrm{pp}}'^2(0)}\right). \quad \text{(A8)}$$

At high field, the Cooperon contribution is already zero, so the crossover function becomes

$$\nu_2(B)=\tfrac{1}{2}\,\frac{\delta g_{\mathrm{ph}}'^2(B)}{\delta g_{\mathrm{ph}}'^2(0)}. \quad \text{(A9)}$$

*Present address: Sandia National Laboratories, Albuquerque, NM 87185.

[1] For a review, see P. A. Lee and T. V. Ramakrishnan, Rev. Mod. Phys. **57**, 287 (1985).

[2] For reviews, see G. Bergman, Phys. Rep. **107**, 1 (1984); or S. Chakravarty and A. Schmid, *ibid.* **140**, 193 (1986).

[3] For a review, see *Mesoscopic Phenomena in Solids*, edited by B. L. Al'tshuler, P. A. Lee, and R. A. Webb (North-Holland, New York, 1991).

[4] C. P. Umbach, S. Washburn, R. B. Laibowitz, and R. A. Webb, Phys. Rev. B **30**, 4048 (1984); J. C. Licini, D. J. Bishop, M. A. Kaster, and J. Melngailis, Phys. Rev. Lett. **55**, 2987 (1985).

[5] R. G. Wheeler, K. K. Choi, and R. Wisnieff, Surf. Sci. **142**, 19 (1984); W. J. Skocpol, L. D. Jackel, R. E. Howard, H. G. Craighead, L. A. Fetter, P. M. Mankiewich, P. Grabbe, and D. M. Tenant, *ibid.* **142**, 14 (1984).

[6] B. L. Al'tshuler, Pis'ma Zh. Eksp. Teor. Fiz. **41**, 530 (1985) [JETP Lett. **41**, 648 (1985)]; P. A. Lee and A. D. Stone, Phys. Rev. Lett. **55**, 1622 (1985).

[7] P. A. Lee, A. D. Stone, and H. Fukuyama, Phys. Rev. B **35**, 1039 (1987).

[8] A. D. Stone, Phys. Rev. B **39**, 10 736 (1989).

[9] S. Feng, Phys. Rev. B **39**, 8722 (1989).

[10] Y. Imry, Europhys. Lett. **1**, 249 (1986).

[11] B. L. Al'tshuler and B. I. Shklovskii, Zh. Eksp. Teor. Fiz. **91**, 220 (1986) [Sov. Phys. JETP **64**, 127 (1986)].

[12] K. A. Muttalib, J.-L. Pichard, and A. D. Stone, Phys. Rev. Lett. **59**, 2475 (1987); P. A. Mello, *ibid.* **60**, 1089 (1988).

[13] C. W. J. Beenakker, Phys. Rev. Lett. **70**, 1155 (1993); Phys. Rev. B **47**, 15 763 (1995).

[14] E. P. Wigner, Ann. Math. **53**, 36 (1953); **62**, 548 (1955); **65**, 205 (1957); **67**, 325 (1958).

[15] F. J. Dyson, J. Math. Phys. **3**, 140 (1962); **3**, 166 (1962); F. J. Dyson and M. L. Mehta, *ibid.* **4**, 701 (1963).

[16] For a review of random matrix theory, see T. A. Brody *et al.*, Rev. Mod. Phys. **53**, 385 (1981).

[17] N. O. Birge, B. Golding, and W. H. Haemmerle, Phys. Rev. Lett. **62**, 195 (1989); Phys. Rev. B **42**, 2735 (1990).

[18] O. Millo, S. J. Klepper, M. W. Keller, D. E. Prober, S. Xiong, A. D. Stone, and R. N. Sacks, Phys. Rev. Lett. **65**, 1494 (1990).

[19] P. Debray, J.-L. Pichard, J. Vicente, P. N. Tung, Phys. Rev. Lett. **63**, 2264 (1989).

[20] V. I. Fal'ko, Pis'ma Zh. Eksp. Teor. Fiz. **53**, 325 (1990) [JETP Lett. **53**, 340 (1991)]; A. A. Bobkov, V. I. Fal'ko, and D. E. Khmel'nitskii, Zh. Eksp. Teor. Fiz. **98**, 703 (1990) [Sov. Phys. JETP **71**, 393 (1990)].

[21] S. Washburn and R. A. Webb, Adv. Phys. **35**, 375 (1986).

[22] A. K. Geim, S. V. Dubonos, and I. Yu, Antonova, Pis'ma Zh. Eksp. Teor. Fiz. **52**, 873 (1990) [JETP Lett. **52**, 247 (1990)].

[23] W. F. Smith, T. S. Tighe, G. C. Spalding, M. Tinkham, and C. J. Lobb, Phys. Rev. B **43**, 12 267 (1991).

[24] See *Amorphous Solids, Low-Temperature Properties*, edited by W. A. Phillips (Springer, New York, 1981).

[25] S. Feng, P. A. Lee, and A. D. Stone, Phys. Rev. Lett. **56**, 1960 (1986).

[26] B. L. Al'shuler and B. Z. Spivak, Pis'ma Zh. Eksp. Teor. Fiz. **42**, 363 (1985) [JETP Lett. **42**, 447 (1985)].

[27] G. A. Garfunkel, G. B. Alers, M. B. Weissman, J. M. Mochel, and D. J. VanHarlingen, Phys. Rev. Lett. **60**, 2773 (1988). For review of $1/f$ noise, see M. B. Weissman, Rev. Mod. Phys. **60**, 537 (1988).

[28] The spin-orbit scattering rate is proportional to $Z^{2\sim5}$ (Z is the atomic number) in metals. (The larger exponent holds within a row of the periodic table; the smaller exponent is an average over a wide range of atomic numbers.) See N. Papanikolaou, N. Stefanou, P. H. Dederichs, S. Geier, and G. Bergman, Phys. Rev. Lett. **69**, 2110 (1992); S. Geier and G. Bergmann, *ibid.* **68**, 2520 (1992).

[29] J. S. Moon, N. O. Birge, and B. Golding, Phys. Rev. B **53**, R4193 (1996).

[30] J. C. Licini, G. J. Dolan, and D. J. Bishop, Phys. Rev. Lett. **54**, 1585 (1985).

[31] G. J. Dolan and J. H. Dunsmuir, Physica B **152**, 7 (1988).

[32] J. H. Scofield, Rev. Sci. Instrum. **58**, 985 (1987).

[33] B. L. Al'tshuler and A. G. Aronov, Pis'ma Zh. Eksp. Teor. Fiz. **33**, 515 (1981) [JETP Lett. **33**, 499 (1981)].

[34] N. Papanikolaou *et al.*, Phys. Rev. Lett. **71**, 629 (1993).

[35] P. Mohanty, E. M. Q. Jariwala, and R. A. Webb, Phys. Rev. Lett. **78**, 3366 (1997) and references therein have shown that dilute spins do not cause L_ϕ to saturate as T approaches zero, but

rather produce a log T behavior from the Kondo effect. We cannot distinguish such a weak temperature dependence from saturation, because our experiments are limited to temperatures above 1 K.

[36] V. Chandrasekhar, P. Santhanam, and D. E. Prober, Phys. Rev. B **42**, 6823 (1990).

[37] J. Pelz and J. Clarke, Phys. Rev. B **36**, 4479 (1987).

[38] P. McConville and N. O. Birge, Phys. Rev. B **47**, 16 667 (1993). See also D. Hoadley, P. McConville, and N. O. Birge (unpublished).

[39] C. W. J. Beenakker and H. van Houten, Phys. Rev. B **37**, 6544 (1988).

[40] The calculation of the full crossover function in one dimension was sent to us by S. Feng (private communication).

[41] B. L. Al'tshuler, A. G. Aronov, and D. E. Khmel'nitskii, J. Phys. C **15**, 7367 (1982).

[42] Y. M. Blanter, Phys. Rev. B **54**, 12 807 (1996).

[43] S. Narita, S. Takeyama, W. B. Luo, S. Hiyamizu, K. Nanbu, and H. Hashimoto, Jpn. J. Appl. Phys., Part 2 **20**, L447 (1981).

[44] C. Weisbuch and C. Hermann, Phys. Rev. B **15**, 816 (1977); M. Dobers, K. v. Klitzing, and G. Weimann, *ibid.* **38**, 5453 (1988).

[45] A. Benoit, S. Washburn, C. P. Umbach, R. A. Webb, D. Mailly, and L. Dumoulin, in *Anderson Localization*, edited by T. Ando and H. Fukuyama (Springer-Verlag, Berlin, 1988), p. 346.

[46] This assumption is based on the grounds that the noise measures the properties of a large number of defects, so that even if each individual defect undergoes a change due to the field (either in its dynamics or in its contribution to the conductance noise), the ensemble average changes only due to the UCF symmetries discussed here. The assumption is justified by the data presented in this paper and in our previous studies of UCF-enhanced $1/f$ noise (Refs. 17 and 38).